SOCIETY OF AUTOMOTIVE ENGINEERS, INC.
485 Lexington Avenue, New York 17, N. Y.

AERODYNAMIC CONTROL OF DECELERATION AND RANGE FOR THE LUNAR MISSION

By Brian Pritchard

NASA Langley Research Center
Langley Station, Hampton, Va.

SOCIETY OF AUTOMOTIVE ENGINEERS

National Aeronautics Meeting
April 3-6, 1962
New York, New York

513D

AERODYNAMIC CONTROL OF DECELERATION AND RANGE FOR THE LUNAR MISSION

By E. Brian Pritchard*

NASA Langley Research Center

SUMMARY

The safe return of a vehicle from a lunar mission involves consideration of deceleration, heat, and range control. This paper examines each with the objective of defining desirable types of entry maneuvers and the degree of maneuverability required for the lunar mission.

Two types of vehicle control, variable-pitch and variable-roll, are analyzed.

The ranges obtainable under optimum conditions are compared with those obtained from pilot simulator studies. It is found that artificial damping about all three vehicle axes is necessary to achieve acceptable range control, although successful entries may be achieved in its absence.

A vehicle, having an L/D capability of 1/2, without aerodynamic controls (i.e., utilizing the roll control mode with reaction jets) is an adequate solution to the problem of safe reentry from a lunar mission if an entry corridor 35 miles in width is acceptable.

INTRODUCTION

The safe return of a vehicle from a lunar mission involves primary consideration of deceleration loads, heat loads, and longitudinal and

---

*Aerospace Technologist.

lateral range attainable from any atmospheric entry point within the reentry corridor. That such a mission is feasible has been shown by many previous investigators (refs. 1 to 24). These researches have been primarily directed towards study of the two prime survival factors - deceleration and heating. Prior to the study conducted by Becker et al. (ref. 25) few investigators had considered the problem of maneuvering a vehicle to a particular destination from any point in the reentry corridor.

Deceleration and heating will be briefly considered here, primarily to demonstrate the effectiveness of aerodynamic maneuvering in reducing the magnitude of such loads. Aerodynamic maneuvers associated with longitudinal and lateral range control will be studied with the objective of defining the more desirable reentry maneuvers for a typical lunar vehicle. The skipping reentry mode will also be considered to determine the effectiveness of extra-atmospheric trajectories in range control.

Primary emphasis has been placed on a vehicle having a maximum lift-drag ratio of 1/2 and a weight parameter $\frac{W}{C_D A}$ of 50 lb/sq ft. Various maneuvers will be studied and compared as to the ranges attainable for a vehicle of this type. Vehicle guidance has been considered primarily in an attempt to provide, in a preliminary way, the answer to two questions: Can a human pilot perform the maneuvers considered here? and can a human pilot achieve the maximum and minimum longitudinal ranges attainable by the methods described here?

SYMBOLS

A	reference area
C_D	drag coefficient based on A
C_L	lift coefficient based on A
D	drag, component of resultant force along flight path
g	acceleration due to gravity at earth's surface
G	resultant acceleration, $\frac{D}{W/g}\sqrt{1 + (L/D)^2}$
h	altitude
l	lateral range measured normal to initial entry plane
L	lift, component of resultant force normal to flight path
m	mass
q	dynamic pressure, $\rho V^2/2$
r_e	mean radius of earth
R	range
t	time
V	velocity
$\overline{V}$	$\sqrt{\frac{V^2}{gr_e}}$
$\overline{V}_i$	V at the end of initial pull-up and start of range-control maneuver
$\overline{V}_o, \overline{V}_f$	values at start and end of constant q transition maneuver (defined on fig. 5)
W	gross weight of vehicle

γ path angle with respect to horizontal

γ_i reentry path angle at 400,000-foot altitude

ρ atmospheric density

ϕ roll angle (zero for unbanked vehicle)

ϕ_1 roll angle at start of range-control maneuver

TYPICAL ENTRY

Two types of reentry trajectories were considered for the lunar mission: "uncontrolled" and "controlled." In the so-called "uncontrolled" reentry, as shown in figure 1, the vehicle enters the atmosphere at a trimmed attitude and maintains this value of L/D throughout the reentry period. The only control allowable is that the trim attitude and hence the L/D may be selected and set prior to entry into the atmosphere. This mode of reentry generally involves large skips outside the atmosphere as indicated.

The "controlled" reentry trajectory indicated in figure 1 is one in which the vehicle attitude is varied to maintain control over the trajectory. For instance, the trajectory may be controlled so as to reduce the peak deceleration and to land the vehicle at a preselected point.

UNCONTROLLED REENTRY

A systematic survey was conducted of vehicles which maintain a fixed lift-drag ratio during the reentry period. If a 10g deceleration

limit is chosen for the undershoot boundary and a maximum skip apogee of 400 miles is taken as the overshoot boundary to avoid the inner radiation belts, a severe restriction is placed on the usable vehicle L/D as shown in figure 2. Here it is seen that the L/D cannot exceed 0.48. Also, the maximum reentry corridor width is approximately 15 miles and occurs at an L/D of 0.2. Another very serious limitation for this type of reentry is the range dispersion, of the order of 1,000 miles, resulting from uncertainties of atmosphere, vehicle aerodynamics, and initial atmospheric entry point. Therefore, it is concluded that control over the reentry trajectory must be utilized if reasonable range control is to be attained.

MODULATED REENTRY PULL-UPS

The reentry corridor may be extended on the lower side if control of the vehicle is utilized during the initial pull-up to reduce the maximum deceleration load during this critical reentry period, i.e., a steeper reentry path is permissible for a given g limit. On the upper side, the corridor can be widened somewhat by use of negative lift initially, followed by a roll maneuver and variable positive lift. It was found that using the maximum modulation technique to reduce g loads had appreciable effect on the range control maneuvers initiated after pull-up.

There are two ways in which the g schedule and reduction of peak g may be accomplished: by variation of the vehicle pitch attitude

or by variation of vehicle geometry. In general, much larger changes in vehicle geometry than have been considered practical are necessary to achieve the same peak g reduction as that obtained by modulation of the vehicle attitude. Grant's method of attitude modulation (ref. 7) is comparatively simple and may be controlled either by the pilot or automatically. In figure 3, this method has been utilized to reduce the peak deceleration load for a vehicle having a lift-drag ratio of 1/2, entering the atmosphere at the attitude for maximum lift coefficient.

In the example shown here a maximum g load of 12.9g's is obtained if no control over the vehicle attitude is exercised. The peak g load may be decreased by modulation of vehicle attitude from that for maximum lift towards that for minimum drag. If it is desired to reduce the maximum g to 10, it is necessary to modulate the lift from $C_{L_{max}}$ to $(L/D)_{max}$. A maximum decrease in maximum g from 12.9 to 7 is obtainable by modulation to $C_{D_{min}}$.

The effect of attitude modulation on the reentry trajectory is indicated by the altitude range curve of figure 3. It is seen that attitude modulation results in the vehicle diving deeper into the atmosphere, producing a decrease in velocity. For instance, the velocity at the bottom of the pull-up is about 30,000 ft/sec for the unmodulated case as compared to 28,000 ft/sec for the maximum modulation case. This results in drastic range capability reductions for maximum modulation and also in some aggravation of the heating problem. It is thus concluded that maximum modulation should be utilized only for emergency

reentry conditions. Modulation from $C_{L_{max}}$ to $(L/D)_{max}$ has been selected as the practical limit for the attitude modulation technique.

REENTRY CORRIDOR BOUNDARIES

The trajectory characteristics during the initial entry pull-up obviously have a significant influence on the entrance angle limits for a single pass entry. Figure 4 indicates the reentry corridor overshoot and undershoot boundaries obtainable for various initial entry maneuvers. For a 10g limited undershoot boundary the maximum benefits of lift for unmodulated entry are realized at an L/D of 1/2. It is seen that modulation of vehicle lift and drag to reduce the resultant deceleration loads yields much higher available entry angles than for the uncontrolled case. For the practical modulation case appreciable benefits occur only for L/D greater than about 1/2.

The three overshoot boundaries shown are somewhat dissimilar in nature. For the uncontrolled case with a skip limitation of 400 miles only a very narrow corridor is available and that for $L/D < 0.48$. A much deeper corridor is available for a vehicle which has the capability of maneuvering to prevent or control the skip after initial entry at $+(L/D)_{max}$. A still greater corridor width is attainable for a vehicle utilizing maximum negative lift during the initial reentry maneuver to avoid a skip outside the atmosphere.

For a vehicle capable of operating from $C_{D_{max}}$ to $C_{D_{min}}$ on its drag polar, the optimum corridor boundaries are indicated by the practical modulation undershoot boundary and the negative $C_{L_{max}}$ overshoot boundary. However, the hypothetical lunar spacecraft considered here is a

vehicle which is trimmed such that it is capable of operation only at maximum lift-to-drag ratio. Reentry maneuvers are obtainable by the roll control mode wherein reaction jets will be utilized. Therefore, in the present range study for a typical lunar vehicle the undershoot limit is taken as the constant L/D curve of figure 4. Although the negative $C_{L_{max}}$ boundary is practical, this paper has considered the +L/D boundary as an operational overshoot boundary for the range control study of a vehicle returning from a lunar mission. The resultant operational reentry corridor is about 35 miles in width. This appears to be quite adequate from the viewpoint of midcourse guidance and control during the lunar mission. This allows for an extended reentry corridor to be utilized if emergency conditions exist wherein range control will not be as important as survival.

AERODYNAMIC MANEUVERS FOR RANGE CONTROL

The longitudinal and lateral distance traversed by a vehicle during reentry is dependent on many variables: entry velocity, entry angle γ_i, L/D, $\frac{W}{C_D A}$, orbit direction, the earth's rotation and oblateness, and atmospheric disturbances. For this study only initial entry conditions have been considered for a vehicle having an L/D of 1/2 and a value of $\frac{W}{C_D A}$ of 50 lb/sq ft. The maximum range control maneuver is considered to be initiated at the velocity $\bar{V}_1$ existing at the end of the pull-up to the desired maneuver flight path as shown in figure 5.

Roll Maneuver

A typical lunar vehicle will probably use only a roll maneuver to control the reentry flight path. An example of the use of this maneuver is presented in figure 6. Here the vehicle is required to maintain a constant altitude trajectory initiated either at the bottom of the initial pull-up or at some later time. For this case, the vehicle must be rolled to produce negative lift if the velocity is greater than circular velocity, zero lift at circular velocity, and positive lift for velocities less than the circular value. Obviously, large lateral ranges are obtainable if the vehicle is always rolled in the same direction. The lateral range aspect of this maneuver is discussed in some detail in the lateral range section of this paper.

Maximum Range

A wholly atmospheric maneuver which yields maximum longitudinal range is difficult to define. It is felt, however, that the constant L/D equilibrium glide is a reasonable approximation. It is necessary to modify this maneuver in the vicinity of $\overline{V} = 1$ since a discontinuity exists in the equations of motion wherein the vehicle's altitude approaches infinity as its velocity approaches the circular value. For the initial phase of this maneuver $\left(\overline{V}_1 \text{ to } \overline{V}_2\right)$ the vehicle flies at negative $(L/D)_{max}$. This is joined to the positive $(L/D)_{max}$ equilibrium glide path by a constant dynamic pressure q maneuver, $\left(\overline{V}_2 \text{ to } \overline{V}_3\right)$. This transitional phase is dictated by the necessity of maintaining adequate

aerodynamic control. It is assumed here that a value of $\frac{1}{w/A} \geq 0.2$ satisfies this condition.

Constant dynamic pressure may be maintained during the transitional maneuver in one of two ways: by rolling the vehicle at fixed pitch such that the lift vector is directed in the appropriate direction to maintain constant dynamic pressure and hence constant deceleration or by varying the pitch angle which incidentally maintains only constant dynamic pressure and not constant deceleration. The fixed-pitch roll maneuver was chosen in this study since this mode could be flown by a pilot without additional instruments other than an onboard accelerometer.

The maximum range attainable from the point where the initial pull-up crosses the equilibrium glide path for this maximum range maneuver is

$$\frac{R}{r_e(L/D)} = \frac{1}{2}\left[\log_e\left(\frac{1 - \bar{V}_1^2}{1 - \bar{V}_2^2}\right) + \log_e\left(\frac{1}{1 - \bar{V}_3^2}\right) + 2\right] \qquad (1)$$

It should be noted that the maximum range was obtained for $\cos \phi = 1$ in the glide phases of the maneuver.

The abrupt changes in flight path shown in figure 5 for this maneuver are of course impossible to achieve. The type of maneuver necessary to change from one path to another has not been considered here but represents a further field of study to be investigated.

Constant Altitude Maneuver

Considerably shorter ranges are obtained by the constant altitude maneuver in comparison with the constant L/D glide. However, it appears to be more desirable from a guidance and control standpoint.

This maneuver has no discontinuity at $\overline{V} = 1$ and for the roll control mode the necessary vehicle bank angle is obtainable by equating the lift force to the sum of the gravity and centrifugal forces. The range equation for the constant altitude portion of reentry may then be written as

$$\frac{R}{r_e(L/D)} = \frac{\cos \phi_1 \overline{V}_1^2}{\left(1 - \overline{V}_1^2\right)} \log_e\left(\frac{\overline{V}_1}{\overline{V}_3}\right) \tag{2}$$

Initiating a constant L/D equilibrium glide at the end of the constant altitude mode yields, for the total range from the point where the constant altitude maneuver is started to impact

$$\frac{R}{r_e(L/D)} = \frac{\cos \phi_1 \overline{V}_1^2}{\left(1 - \overline{V}_1^2\right)} \log_e\left(\frac{\overline{V}_1}{\overline{V}_3}\right) + \frac{1}{2} \log_e\left(\frac{1}{1 - \overline{V}_3^2}\right) \tag{3}$$

In order to evaluate the comparative effects of using either the roll control maneuver or the pitch control maneuver to maintain constant altitude, the nonintegrable equations of motion for the pitch control case were solved by numerical integration on a high-speed digital computer. These results were obtained for a flat-bottomed vehicle assuming that Newtonian force relationships apply.

Minimum Range

True minimal ranges may be defined only by a quite complex variable lift maneuver which must be initiated immediately upon the vehicle's entry into the atmosphere. For this reason an approximate method was used here to obtain minimum ranges which are felt to be quite close to the true values.

Approximate minimum ranges were obtained by assuming a constant 10g deceleration from the point of peak g during the initial entry pull-up. Fixed-pitch roll control was utilized such that constant dynamic pressure and hence constant g load could be maintained. Obviously a constant 10g trajectory could not be maintained to impact with the earth. However, the velocity at which a 10g deceleration can no longer be maintained is quite small in comparison with the initial velocity and is therefore assumed to be zero. The range equation for this maneuver is

$$\frac{R}{r_e} = \frac{\sqrt{1 + (L/D)^2}\, V_{g_{max}}^2}{20} \tag{4}$$

Controlled Skip

It is desirable to compare the maximum range attainable by a wholly atmospheric maneuver with a maneuver which is controlled to allow a skip to an altitude of 400 miles. In this maneuver constant altitude is maintained at the initial pull-up point until sufficient kinetic energy has been dissipated such that when the vehicle is rolled to $\phi = 0$ the desired skip will result. Digital computer results were used to obtain the range for this controlled skip maneuver.

A complete derivation of the range equations for these atmospheric reentry maneuvers may be found in reference 25.

LONGITUDINAL RANGE

The ranges obtained with the atmospheric maneuvers considered here are compared in figure 7 as a function of the velocity at which the maneuver is initiated for a vehicle having a maximum L/D capability of 1/2. Also shown is the initial value of the resultant deceleration, G_1. For the higher initial velocities the constant L/D equilibrium glide maneuver yields much longer ranges than the constant altitude maneuver. The constant altitude mode results in increasing range with decreasing initial velocity, since the deceleration level is lower for the lower velocities, more than offsetting the decrease in initial kinetic energy level. Considerable range increase is attainable by utilization of the variable-pitch maneuver rather than the variable-roll maneuver since the variable-pitch maneuver operates on a Newtonian drag polar between C_D for $(L/D)_{max}$ and $C_{D_{min}}$; resulting in the vehicle flying at a much lower deceleration level than for the variable-roll maneuver which operates continuously at C_D for $(L/D)_{max}$.

The longitudinal range attainable for an $(L/D)_{max} = 1/2$ vehicle from the point of initial entry into the atmosphere is shown in figure 8. As is to be expected, the controlled skip reentry maneuver yields by far the greater longitudinal ranges. Unfortunately, this mode is critically dependent on the velocity and path angle at which the skip is initiated.

Reference 25 points out that this mode is too susceptible to large uncorrectable range errors to be considered a reliable method of range control. The maximum range, constant L/D glide maneuver yields ranges of the order of 6,000 miles near the undershoot limit which appears adequate for the reduced reentry corridor utilized in this study. The constant altitude (type B) curve is obtained by initiating constant altitude at the same point as the constant L/D glide and the constant altitude (no skip) curve is obtained by maintaining constant altitude at the bottom of the initial pull-up for as long as possible. Both of these maneuvers yield comparatively low ranges near the undershoot boundary.

The minimum indicated ranges were obtained by use of the constant 10g deceleration maneuver. The available range overlap is defined as the difference between the maximum range attainable at the undershoot boundary and the minimum range attainable at the overshoot boundary. Here the longitudinal range overlap is shown to be approximately 4,000 miles using the constant L/D equilibrium glide maneuver for maximum range or 3,000 miles using the type B, fixed-pitch variable roll constant altitude maneuver. It is easily seen that the optimum maximum range maneuver must involve a pull-up to regions of comparatively low density followed by either the constant L/D equilibrium glide maneuver or a constant altitude maneuver. A choice between these two maneuvers must depend on the pilot's ability to execute practical approximations to these idealized maneuvers. This is, of course, also dependent on the choice of the vehicle control system. Currently, the leading

candidate is the simplest possible approach: roll control only with the fixed-pitch attitude for maximum L/D controlled by the center-of-gravity location.

It should also be noted from figure 8 that reducing the design operational reentry corridor width will result in increased range overlap.

It is concluded that the performance of the L/D = 1/2 vehicle, operating in the reentry corridor considered here, is adequate for the safe return of the vehicle from a lunar mission.

LATERAL RANGE

Many previous studies of lateral range (refs. 18, 19, and 26) have been primarily concerned with satellite reentry wherein most of the lateral range is attained after the vehicle has reached comparatively low velocities. In general, the lateral range traversed is small and the sphericity of the earth can be neglected.

This is not generally the case for parabolic reentry velocities however. Regions of high dynamic pressure are reached during the initial pull-up and large changes in heading angle may be attained. The much larger lateral ranges thus available require consideration of the earth's sphericity. The complete equations of motion including spherical effects developed in reference 25 necessitate numerical integration on a high-speed digital computer. A comparison of the lateral range attainable by both considering and neglecting the earth's sphericity for several values of L/D is shown in figure 9. A middle corridor reentry was

considered for vehicles having a value of $\frac{W}{C_D A} = 50$ lb/sq ft performing normal initial pull-ups followed by the constant L/D equilibrium glide maneuver at various constant bank angles. It is seen that large lateral range errors are introduced by utilization of the cylindrical earth approximation especially at the higher L/D values. Errors of the order of 10 percent occur for the L/D = 0.5 vehicle and would be markedly greater if the controlled skip maneuver were used indicating that even for such low L/D vehicles the sphericity of the earth should not be neglected.

The lateral range attainable by an L/D = 1/2 vehicle utilizing the atmospheric modes previously discussed is presented in figure 10 as a function of the velocity at which the maneuver is initiated. As in the case of longitudinal ranges, the constant L/D equilibrium glide maneuver displays a significant increase in lateral range capability over the constant altitude maneuver. The third curve shown here is the lateral range obtained in reference 27 wherein the vehicle was pilot controlled to a reference trajectory comparable to the constant altitude reentry maneuver considered here. A further discussion of this curve is included in the section on piloted reentry.

The control of lateral range for the constant altitude mode by alternating the sign of the roll angle so as to alternate the direction of the resultant side force is presented in figure 11. As shown here, for a vehicle with L/D = 1/2 disallowing skips out of the atmosphere, maximum lateral range is attained by maintaining the roll angle and

hence the side-force component of the lift vector in the same direction (OABCD). If no resultant lateral range is desired, a minimum of one change in the sign of roll angle is required (OBH) or any number of changes (OAJH). A desired lateral range less than the maximum requires one or more changes in roll angle sign (OBFG or OCE). Obviously, this method of controlling lateral range applies to all the reentry maneuvers considered in this paper as well as the constant altitude maneuver.

AERODYNAMIC HEATING

In the design of a vehicle heat shield it is necessary to have an extensive knowledge of the maximum heating rates and total heat loads which the vehicle will encounter during its entry into the atmosphere. Two types of aerodynamic heating exist: convective and radiative. For reentry at parabolic velocities the radiative heat load is less than about 15 percent of the convective heating and has therefore not been considered here. In figure 12 is shown the maximum stagnation point convective heating rate encountered during reentry as a function of the total heat load for several of the maneuvers considered here. The vehicle in this illustration has an L/D capability of 1/2, a value of $\frac{W}{C_D A}$ of 50 lb/sq ft and a nose radius of 1 foot.

Increasing the maximum g level (approaching the under shoot boundary) results in higher maximum heating rates and lower total heat loads. Also, for a given initial entry condition the constant g reentry maneuver yields lower total heat loads than either the constant altitude

or constant L/D maneuvers. As is to be expected, the constant L/D mode results in maximum total heat loads. This figure once again indicates the superiority of the maneuverable vehicle over the nonmaneuverable vehicle. The heat loads indicated here are well within the capability of proposed heat shields.

PILOTED REENTRY

In consideration of reentry from a lunar mission it is necessary to determine the capabilities of a pilot in flying the reentry maneuvers of interest. Basically, pilot simulation studies (refs. 26 and 27) are concerned with three factors:

1. Ability of the pilot to make the pull-up transition maneuver.

2. Ability of the pilot and the guidance and control system to achieve range control.

3. Optimum instrument displays to facilitate 1 and 2.

The six-degree-of-freedom analog simulator study carried out by Moul, Schy, and Williams utilized the instrument display presented in figure 13 and was concerned with only the first of the above factors. The angle-of-attack meter and "8" ball are used by the pilot to set angles of attack and roll prior to initial entry into the atmosphere. Velocity, altitude, and acceleration are monitored during reentry. It was found in this study that the inclusion of an altitude rate meter in the instrument display was quite helpful in allowing the pilot to successfully pull-up and fly a constant altitude maneuver. (Type B of fig. 5.)

In this study the pilot was required to enter the atmosphere at constant C_L near $(L/D)_{max}$ and pull-up to zero flight-path angle at an altitude of 210,000 feet. Entries considered were: a steep entry near the undershoot boundary; a shallow entry near the overshoot boundary; and a middle corridor entry.

After the pull-up to zero path angle, lift was modulated by the roll-pitch maneuver wherein negative lift is obtained by rolling the vehicle 180°. Constant gain automatic rate dampers were employed for all three axes. A two-axis side-arm controller was used for pitch and roll control and foot pedals for yaw control.

It was found that the pilots considered these three entry types (fig. 14) comparatively simple with all dampers operating after some initial familiarization with the task to be performed. However, entry with all dampers inoperative was considered to be unacceptable except for emergencies where range control is a secondary problem. The type of vehicle used, a blunt-faced, high-drag body with $(L/D)_{max} = 1/2$, is particularly susceptible to aerodynamic control cross coupling. Loss of either the yaw or roll dampers was not considered to render control of the vehicle hazardous.

Foudriat and Wingrove (ref. 28) studied several reentry guidance and control techniques for reentry at parabolic velocities. Among these were: reference trajectory techniques; repetitive prediction techniques; and pilot controlled techniques. In the reference trajectory procedure the control feedbacks were developed for successful operation of the

system. The repetitive prediction system utilized a rapid-time analog computer to predict the range capability from the present conditions. The pilot's intelligence and learning capabilities were used to provide the guidance logic and the control commands in the pilot controlled techniques.

The range capability of each of these techniques is presented in figure 15 for a blunt-faced, high-drag vehicle having an L/D capability of approximately 1/2 and a value of $\frac{W}{C_D A}$ of 50. Here, the minimum and maximum longitudinal ranges have been obtained throughout the reduced reentry corridor previously discussed. The repetitive prediction technique was shown to yield very good control of the initial peak deceleration and hence minimal ranges. In this preliminary study, no attempt was made to approximate any of the particular flight modes analyzed in the present range study. The pilot practiced an arbitrary type of maneuver wherein a pull-up, initiated upon entering the atmosphere, was terminated at an altitude of about 250,000 feet with a velocity varying between 25,000 and 27,000 ft/sec. This is a flight plan most nearly approximated by the equilibrium glide maneuver of the present study. The piloted ranges thus obtained are far short of the theoretical values obtained here using the constant L/D equilibrium glide method. It appears, however, that the velocity at which the coast altitude is reached may be increased with further system refinement and pilot schooling resulting in longitudinal ranges considerably closer to the optimum values obtained here. Further research in this field is presently being pursued at Langley.

As was indicated in figure 10, optimum lateral ranges are more nearly obtainable by present guidance systems than optimum longitudinal ranges. This is primarily due to the fact that full available side force may be used at all times during reentry without regard to skipping out of the atmosphere, as in the case of longitudinal range control. Extension of the present piloted longitudinal ranges will naturally provide some further increase in lateral range.

CONCLUSION

Uncontrolled reentry at fixed L/D is found to be unacceptable for the lunar mission. A maneuverable reentry vehicle is shown to possess a much larger available reentry corridor and relatively good range control. For maximum range control capability the vehicle must be equipped with aerodynamic controls. Such a vehicle, with an L/D capability of 1/2, would have a reentry corridor some 52 miles in width. For nominal design purposes, if a 35-mile corridor depth is used, this vehicle would be able to reach its prescribed destination from any extremity of the reentry corridor with at least a ±1,500-mile-range margin. Utilizing such a reduced reentry corridor eliminates the need for aerodynamic controls if the vertical lift of the vehicle is varied by rolling the vehicle in a fixed-pitch attitude, i.e., by proper choice of the center of gravity such that the vehicle is self-trimmed at the attitude for maximum L/D.

Except in the case of minimum desired ranges, the sphericity of the earth must be considered for lateral range calculations at parabolic reentry velocities.

A human pilot is capable of performing the basic maneuvers required for range control if artificial rate damping about three axes is provided. However, the maximum longitudinal ranges so far obtained in piloted simulator studies are much less than those obtained theoretically. This is due to the kinetic energy lost in the transition between the pull-up and the glide maneuver. With system refinement and pilot training it should be possible to perform this maneuver with considerably more energy, economy, and greater range control.

Finally, it is concluded that a vehicle with an L/D capability of 1/2 is quite adequate for the limited lunar mission requirements.

REFERENCES

1. Chapman, D. R.: An Analysis of the Corridor and Guidance Requirements for Supercircular Entry Into Planetary Atmospheres. NASA TR R-55, 1959.

2. Lees, L., et al.: Use of Aerodynamic Lift During Entry Into the Earth's Atmosphere. ARS Journal 29, No. 9, Sept. 1959.

3. Grant, F. C.: Importance of the Variation of Drag With Lift in Minimization of Satellite Entry Acceleration. NASA TN D-120, 1959.

4. Wong, Kenneth, and Ting, Lu: Analytic Solutions of Planar Reentry Trajectories With Lift and Drag. PIBAL Rept. No. 601, April 1960.

5. Grant, F. C.: Analysis of Low-Acceleration Lifting Entry From Escape Speed. NASA TN D-249, 1960.

6. Crisp, J. D. C., and Feitis, P.: The Thermal Response of Heat-Sink Reentry Vehicles. Polytechnic Institute of Brooklyn (PIBAL) Rept. No. 576, July 1960.

7. Grant, F. C.: Modulated Entry. NASA TN D-452, 1960.

8. Styer, E. F.: A Parametric Examination of Reentry Vehicle Size and Shape for Return at Escape Velocity. Paper presented at Third Annual Meeting, American Astro. Society, Aug. 8-11, 1960.

9. Kelly, O. A., Jr.: Parametric Study of a Manned Space Entry Vehicle. Aero-Space Engineering, 19, No. 10, Oct. 1960.

10. Galman, B. A.: Direct Reentry at Escape Velocity. Paper presented at Third Annual Meeting, Amer. Astro. Soc., Seattle, Washington, Aug. 8-11, 1960.

11. Teague, R.: Flight Mechanics of Reentry After Circumlunar Flight by Means of Various Lifting Techniques. NASA-George C. Marshall Space Flight Center, MNN-M-Aero-4-60, Sept. 15, 1960.

12. Hilderbrand, R. B.: Manned Reentry at Supersatellite Speeds. IAS Rept. No. 60-83, Sept. 1960.

13. Minzner, R. A., et al.: ARDC Model Atmosphere. 1959 Geophysics Research Directorate, ARDC, U.S. Air Force, 1959.

14. Hays, J. E., et al.: Analytical Study of Drag Brake Control System for Hypersonic Vehicles. Wright Air Develop. Div., U.S. Air Force Tech. Rept. 60-267, Jan. 1960.

15. Becker, J. V.: Heating Penalty Associated With Modulated Entry Into Earth's Atmosphere. ARS Journal, 30, May 1960.

16. Bryson, A. E., et al.: Determination of the Lift or Drag Program That Minimizes Reentry Heating With Acceleration or Range Constraints Using a Steepest Decent Computation Procedure. IAS Paper, New York Meeting, Jan. 23-25, 1961.

17. Wingrove, R. C., and Coate, R. E.: Piloted Simulator Tests of a Guidance System Which Can Continuously Predict Landing Point of a Low L/D Vehicle During Atmospheric Reentry. NASA TN D-787, 1961.

18. Slye, R. E.: An Analytical Method for Studying the Lateral Motion of Atmosphere Entry Vehicles. NASA TN D-325, 1960.

19. Mandell, D. S.: A Study of the Maneuvering Performance of Lifting Reentry Vehicles. Paper presented at 15th ARS Annual Meeting, Washington, D.C., Dec. 5-8, 1960.

20. Fridelander, A. L., and Harry, D. P., III: Requirements of Trajectory Convective Impulses During the Approach Phase of an Interplanetary Mission. NASA TN D-255, 1960.

21. Eggleston, J. M., et al.: Fixed-Base Simulator Study of a Pilot's Ability to Control a Winged Satellite Vehicle During High-Drag Variable-Lift Entries. NASA TN D-228, 1960.

22. Adams, Mac C.: A Look at the Heat Transfer Problem at Super-Satellite Speeds. ARS Paper, Annual Meeting, Washington, D.C., Dec. 5-8, 1960.

23. Brumer, M. J.: The Aerodynamic and Radiant Heat Input to Space Vehicles Which Reenter at Satellite and Escape Velocity. ARS Paper presented at ARS 15th Annual Meeting, Washington, D.C., 1960.

24. Allen, H. J.: Problems in Atmospheric Entry From Parabolic Orbits. Paper presented at Conference on Aeronautical and Space Engineering, Nagoya, Japan, Nov. 8-9, 1960.

25. Becker, J. V., Baradell, D. L., and Pritchard, E. B.: Aerodynamics of Trajectory Control for Reentry at Escape Speed. IAA Paper presented at IAA Symposium, Paris, France, June 1961.

26. Jackson, W. Scott: An Improved Method for Determining the Lateral Range of a Gliding Reentry Vehicle. Journal of the Aerospace Sciences, vol. 28, no. 11, Nov. 1961.

27. Moul, M. T., Schy, A. A., and Williams, J. L.: Dynamic Stability and Control Problems of Piloted Reentry From Lunar Missions. NASA TN D-986, 1961.

28. Foudriat, E. C., and Wingrove, R. C.: Guidance and Control During Direct-Descent Parabolic Reentry. NASA TN D-979, 1961.

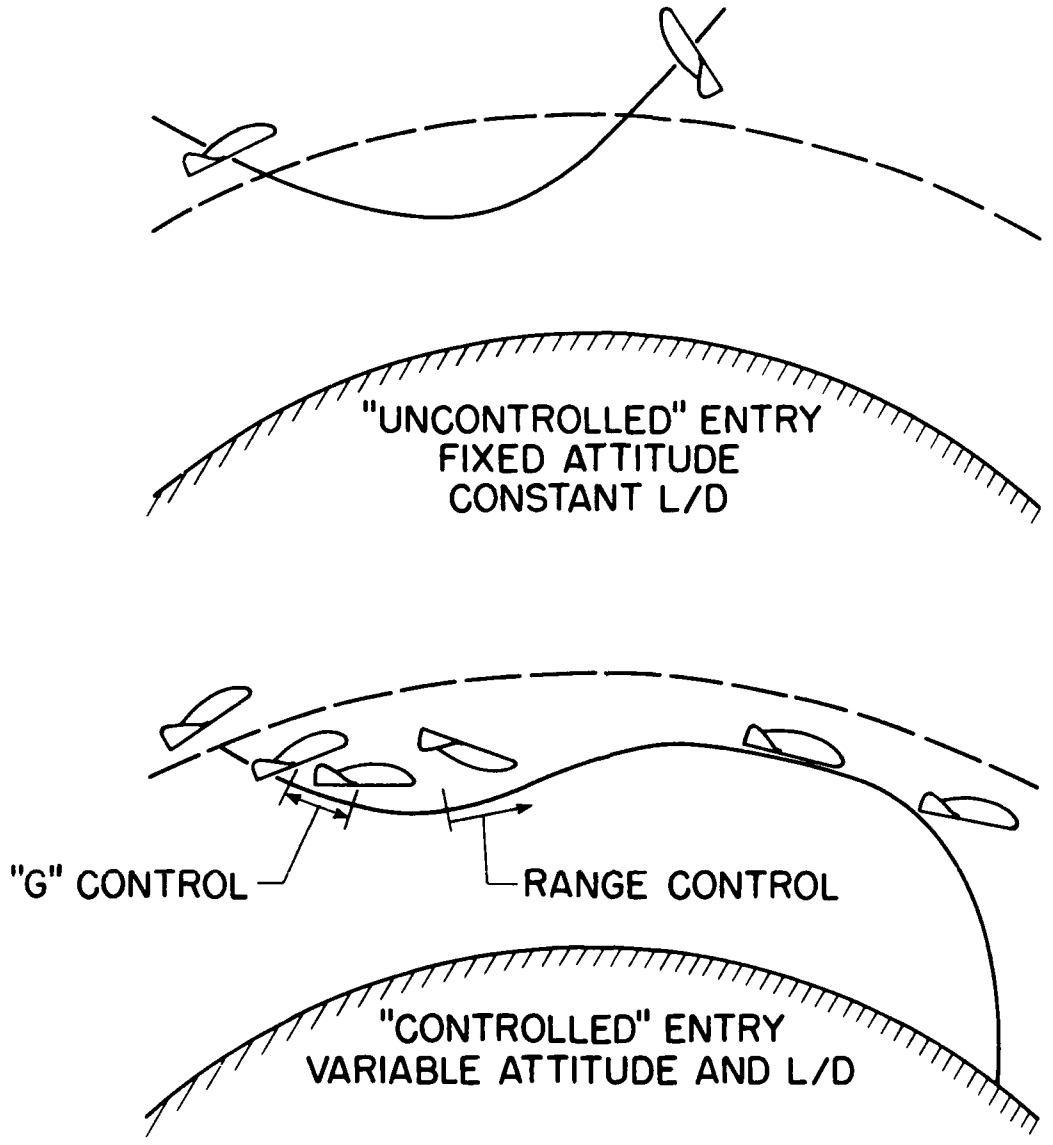

NASA

Figure 1.- Comparison of "Uncontrolled" and "Controlled" entry.

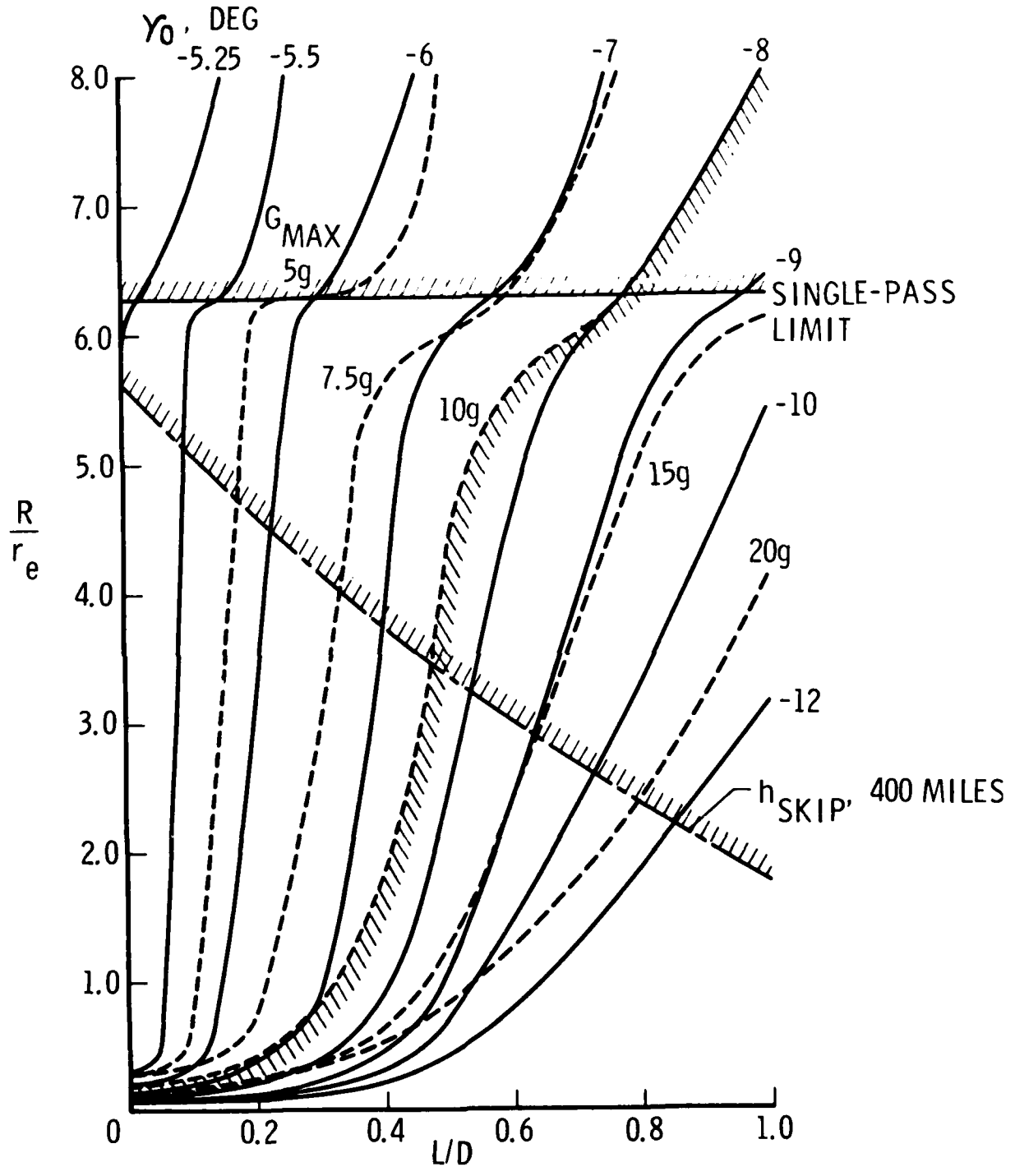

NASA

Figure 2.- Uncontrolled reentries.

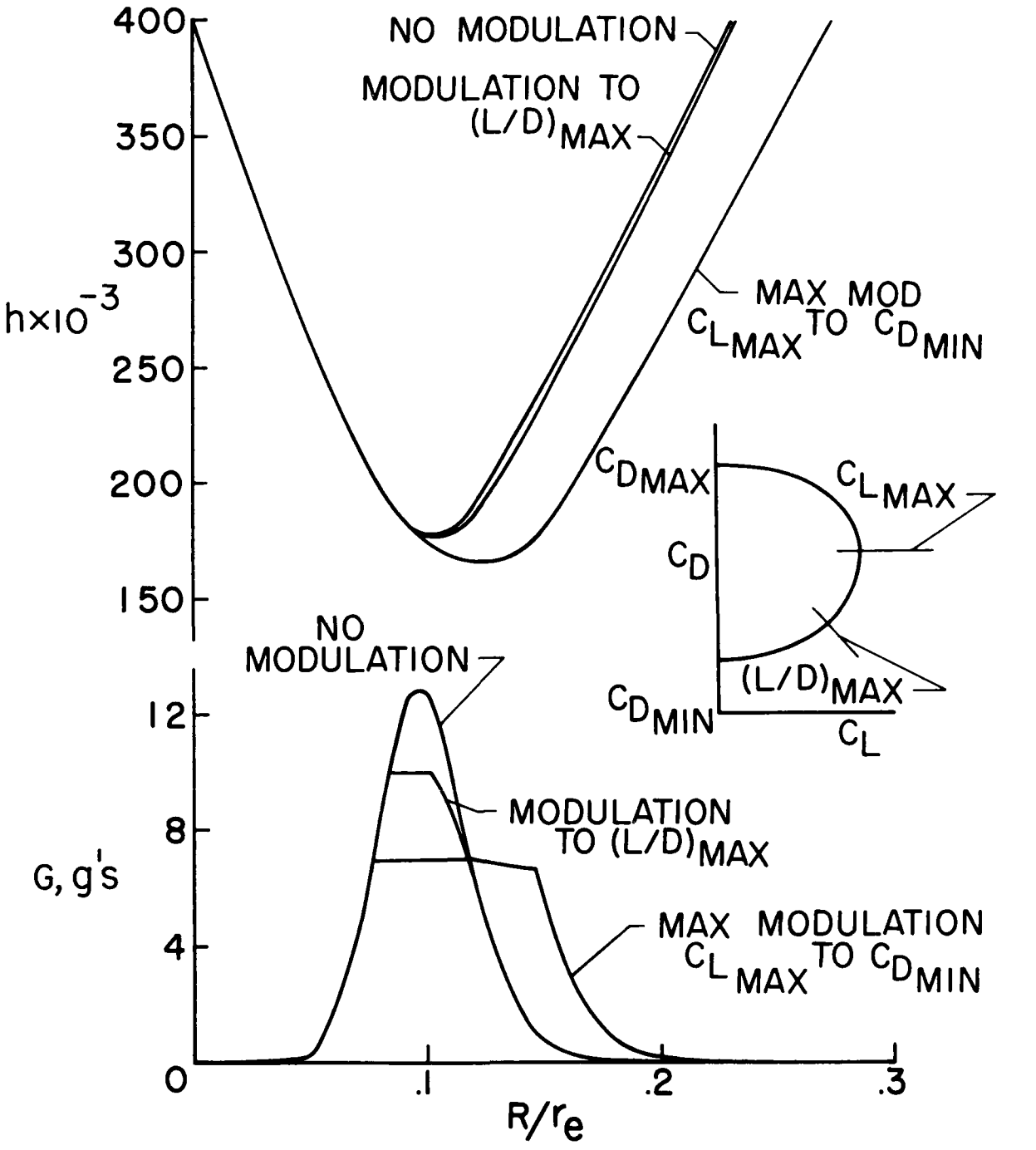

NASA

Figure 3.- Modulated reentry pull-up techniques. $\gamma_i = -8.11^\circ$.

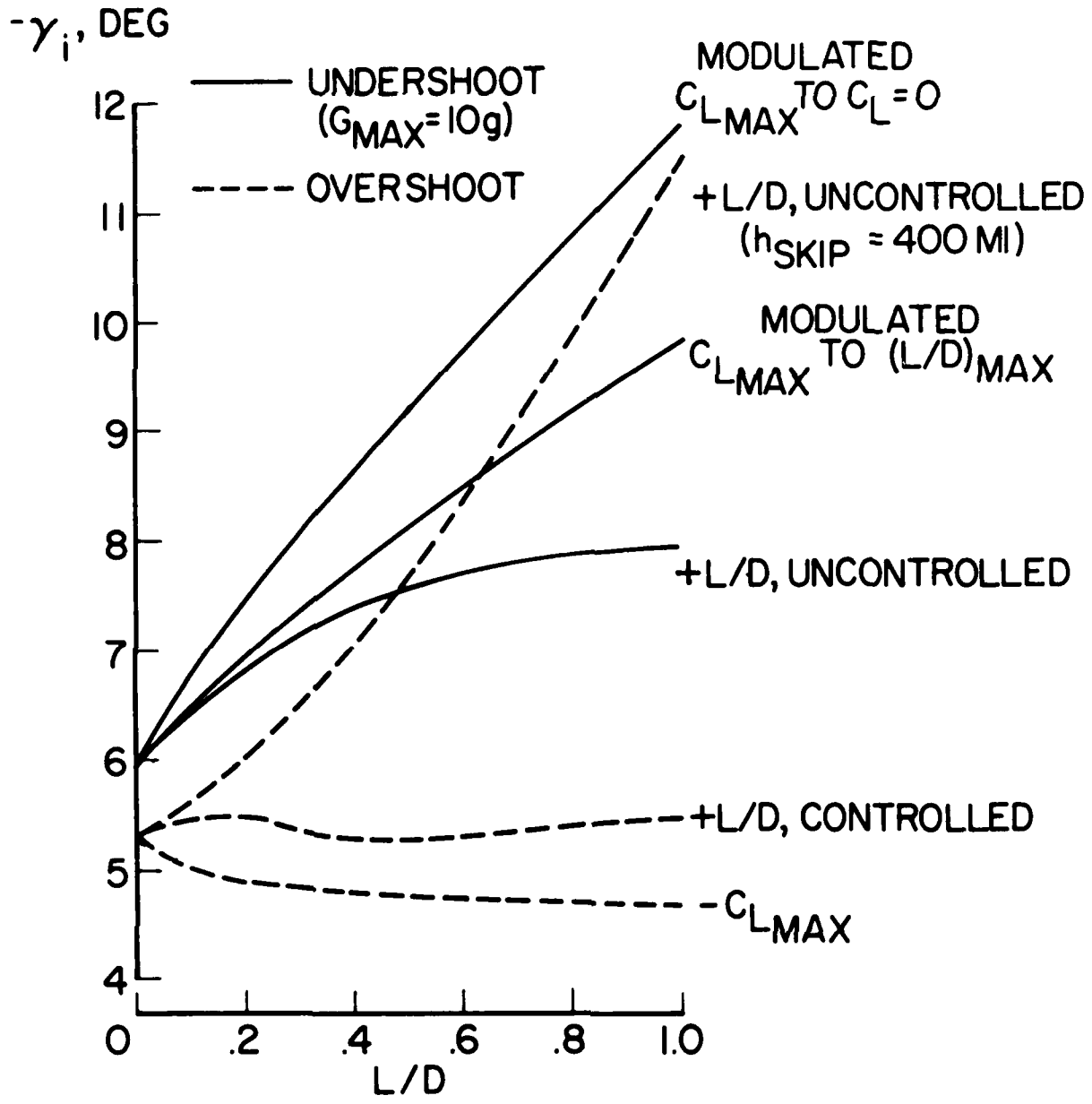

NASA

Figure 4.- Vertical boundaries of reentry corridor as affected by L/D and type of initial reentry maneuver.

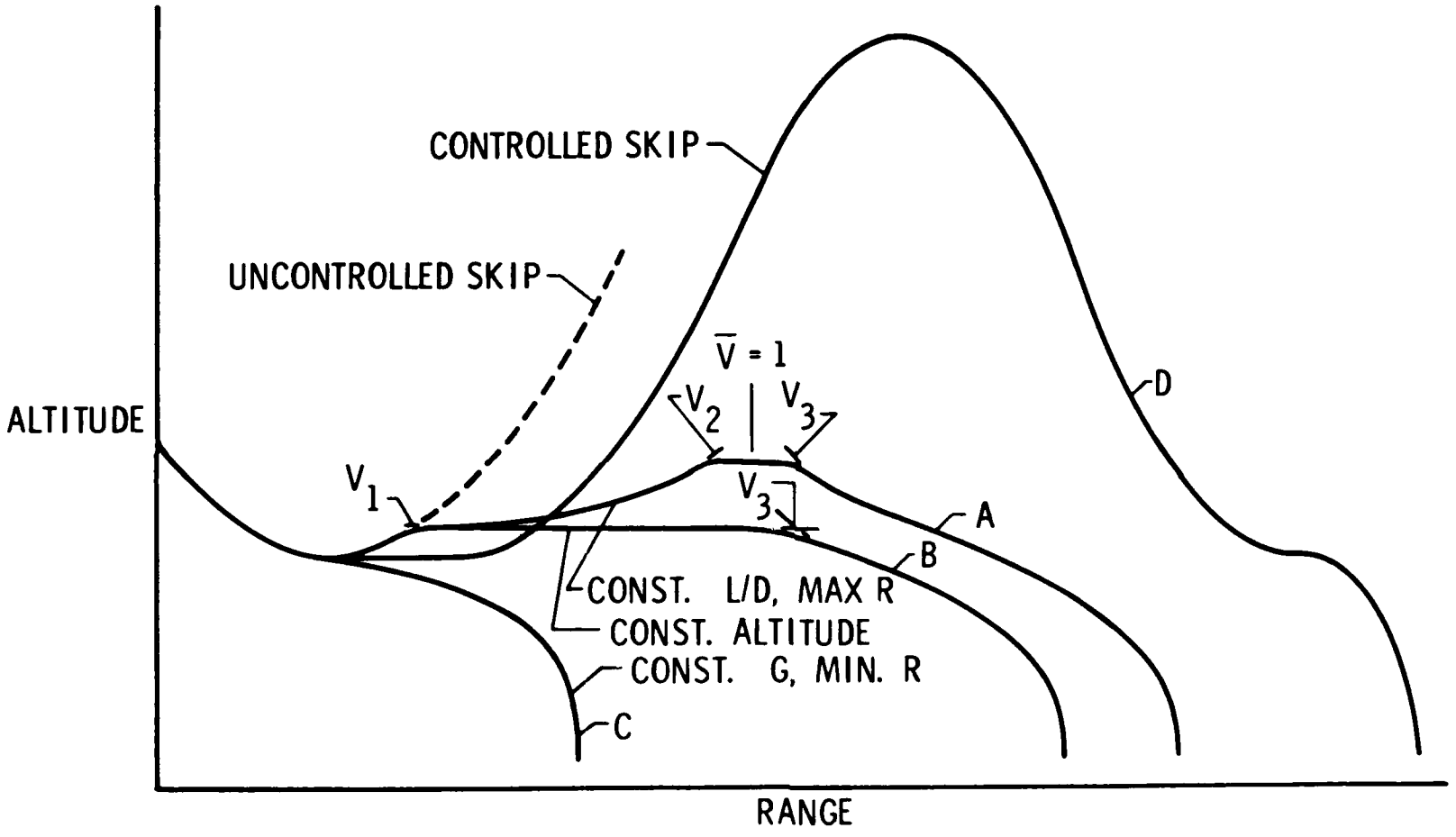

NASA

Figure 5.- Reentry trajectories considered in range study.

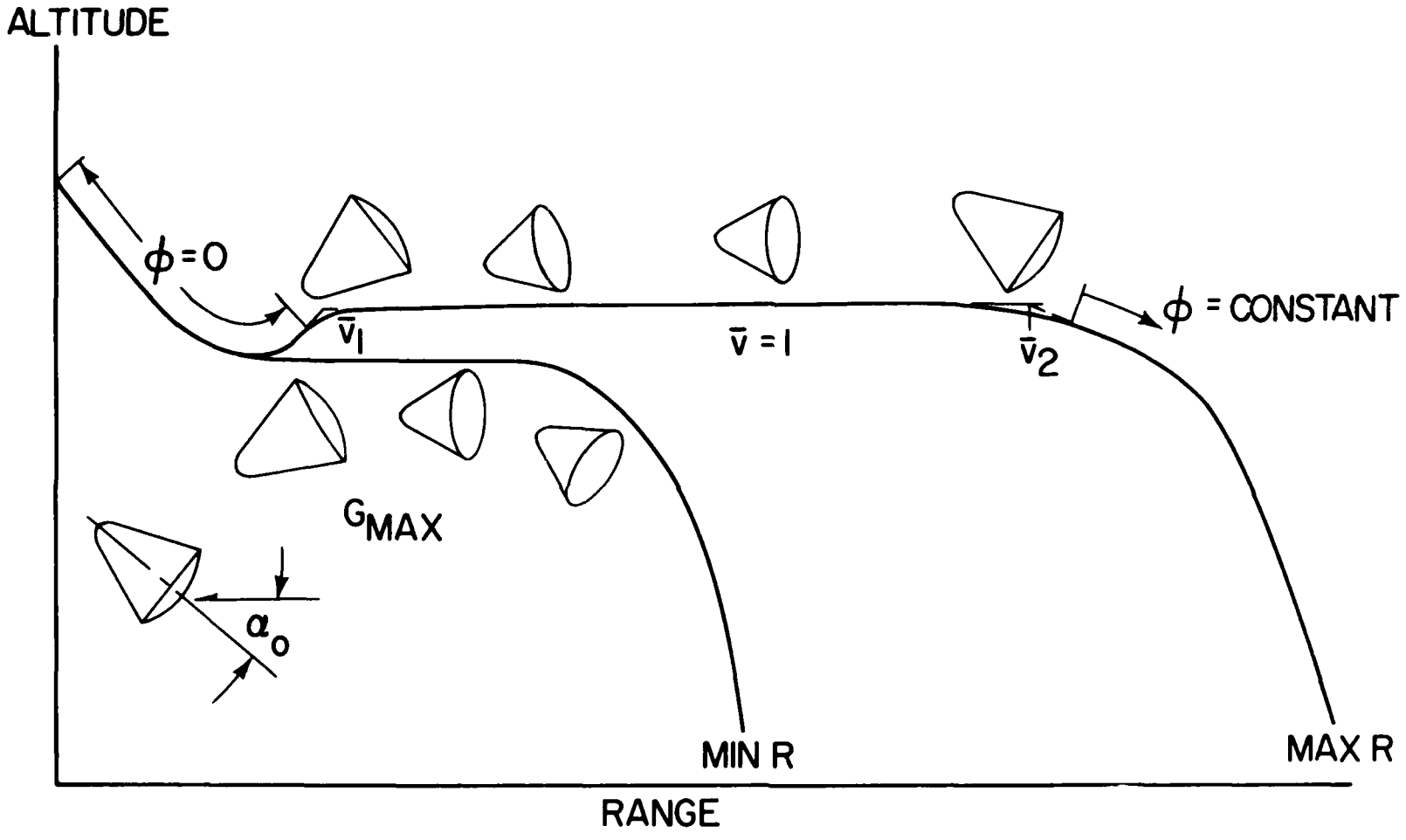

NASA

Figure 6.- Details of variable roll control mode.

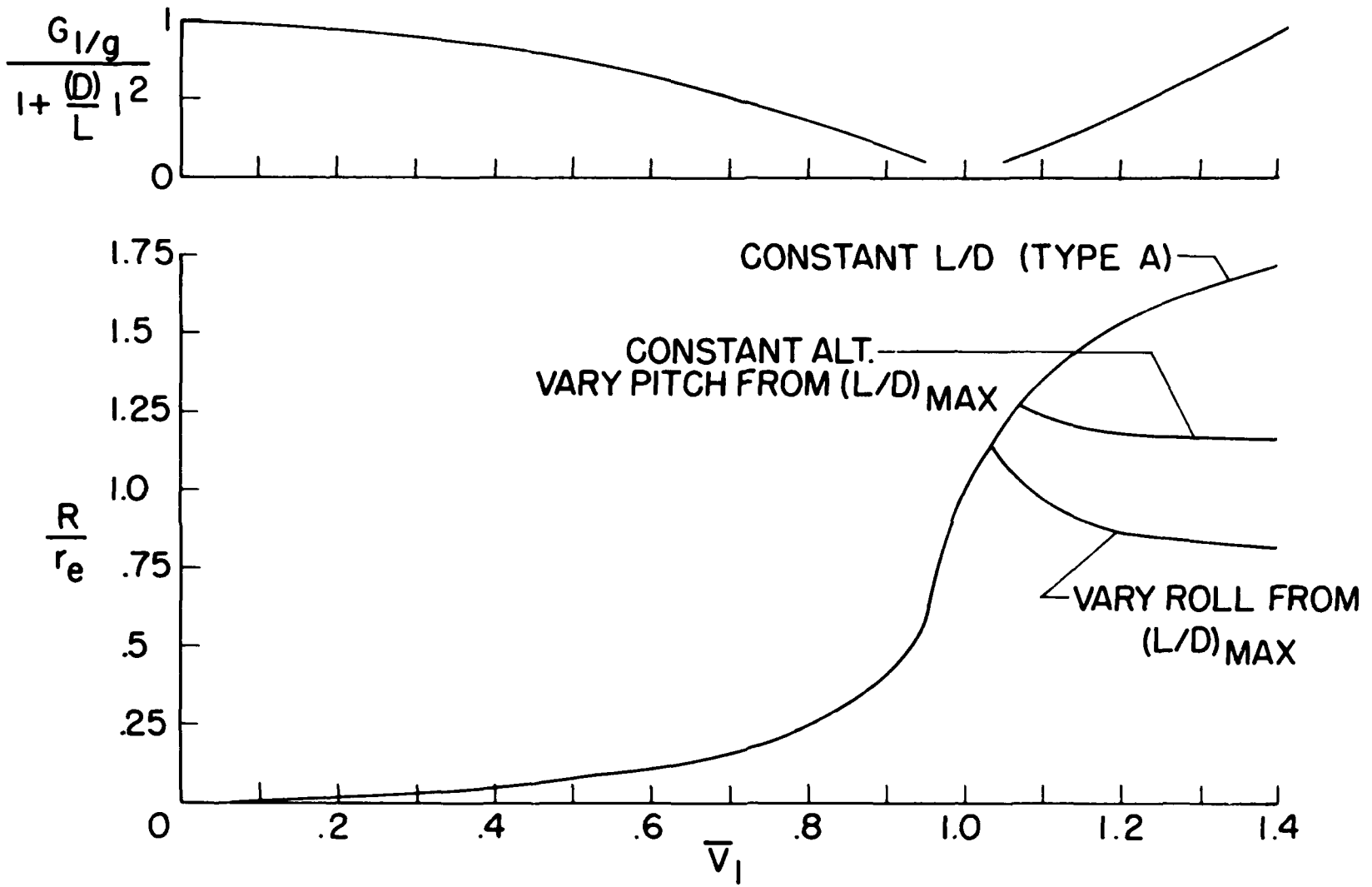

Figure 7.- Comparison of longitudinal range for the various atmospheric modes starting at equal conditions at the end of the initial pull-up maneuver. $(L/D)_{max} = 0.5$.

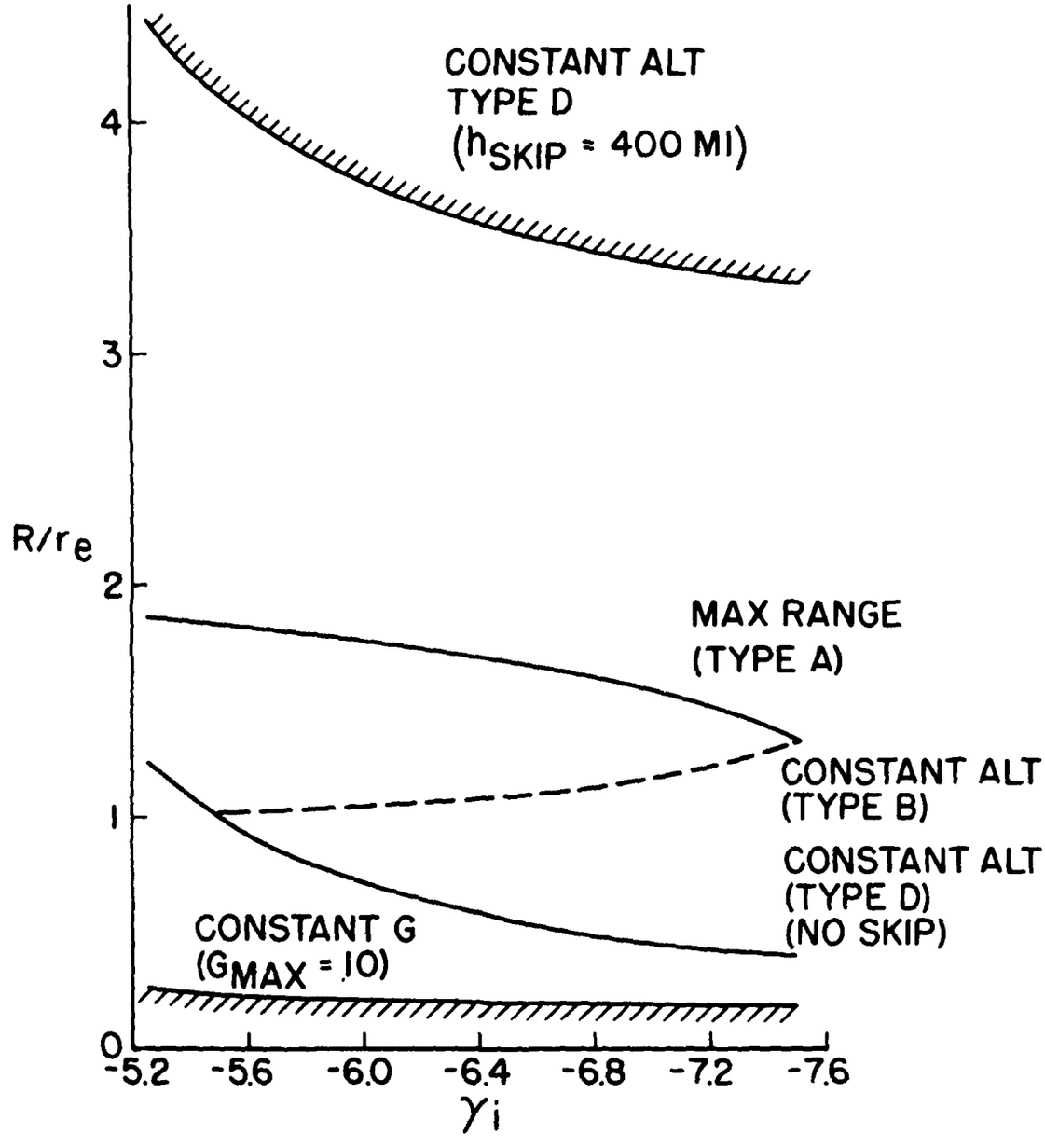

NASA

Figure 8.- Comparison of longitudinal range for atmospheric and controlled skip modes. $(L/D)_{max} = 0.5$.

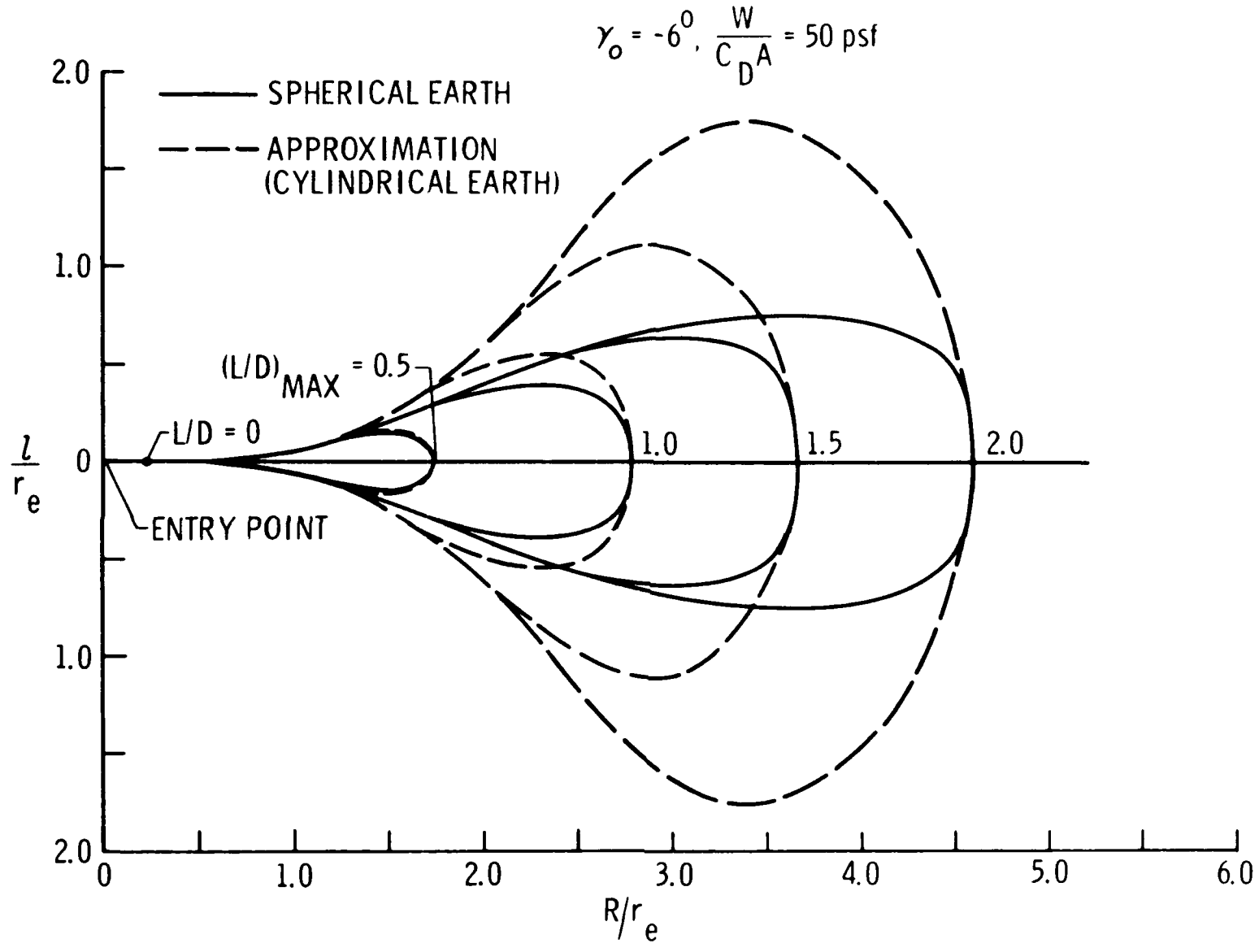

Figure 9.- Available landing area for maximum range mode.

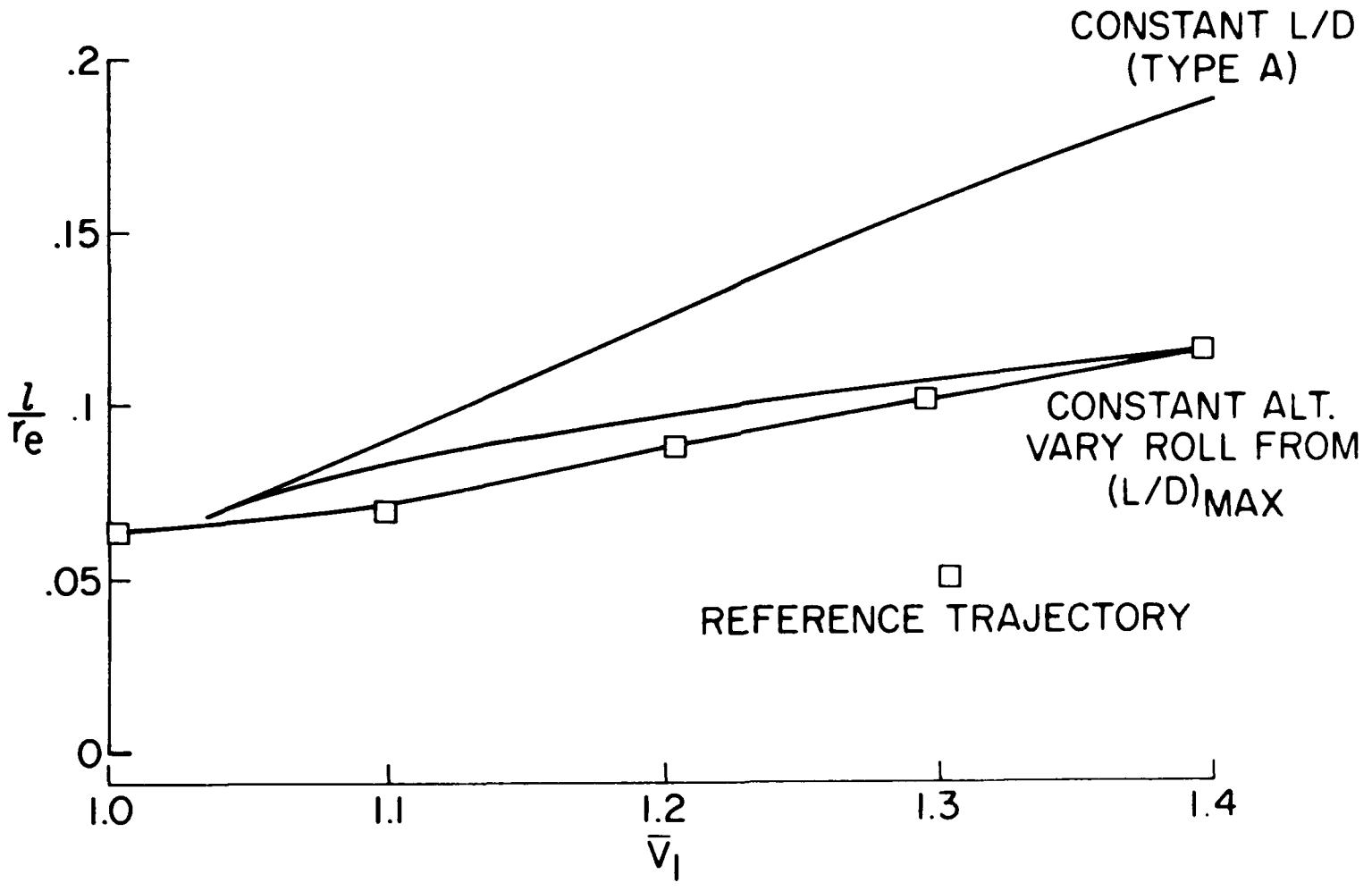

NASA

Figure 10.- Comparison of lateral range for atmospheric modes. $(L/D)_{max} = 0.5$.

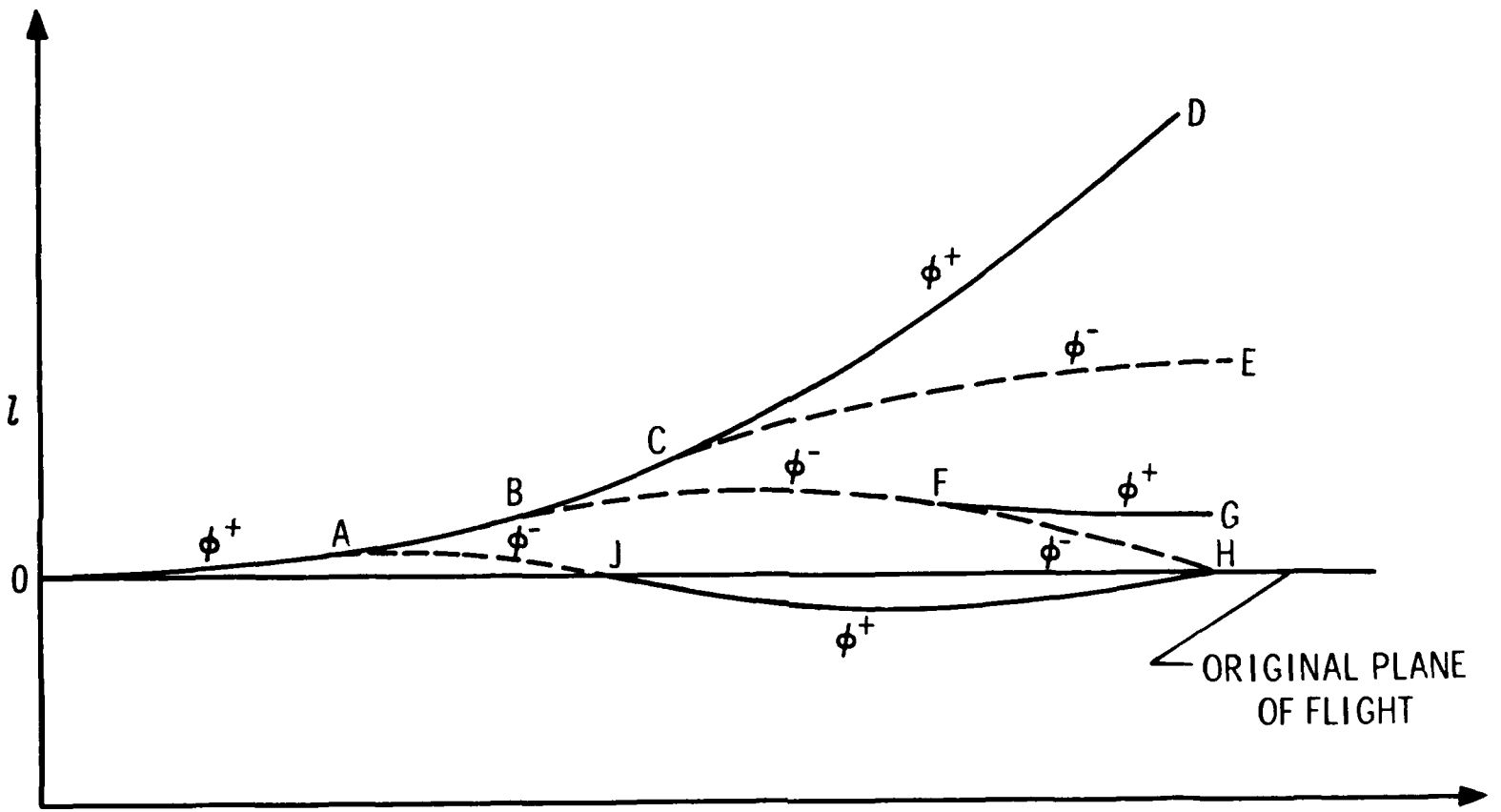

NASA

Figure 11.- Control of lateral range for the constant altitude mode.

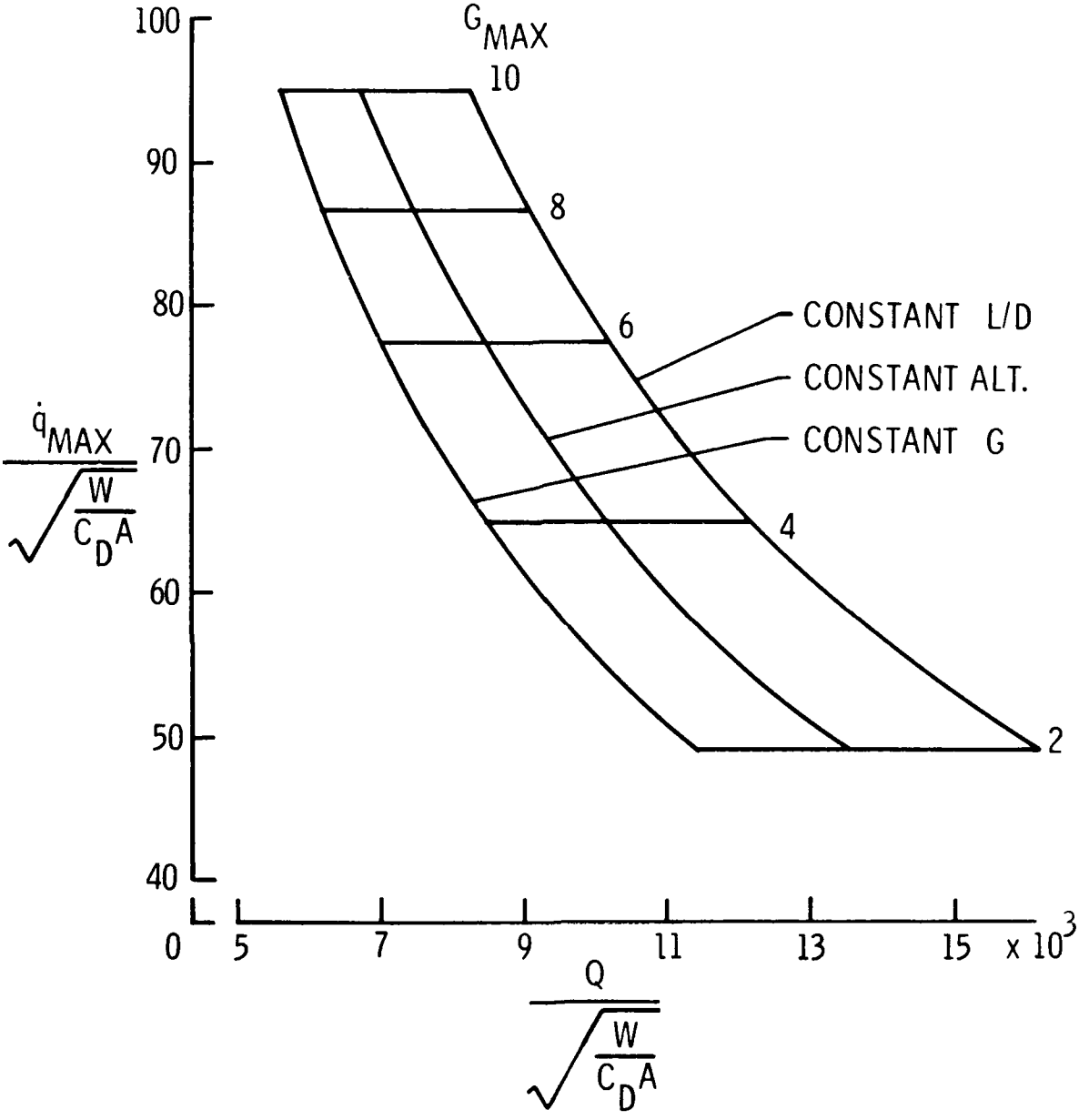

NASA

Figure 12.- Convective heat loads as affected by reentry mode. (L/D = 0.5.)

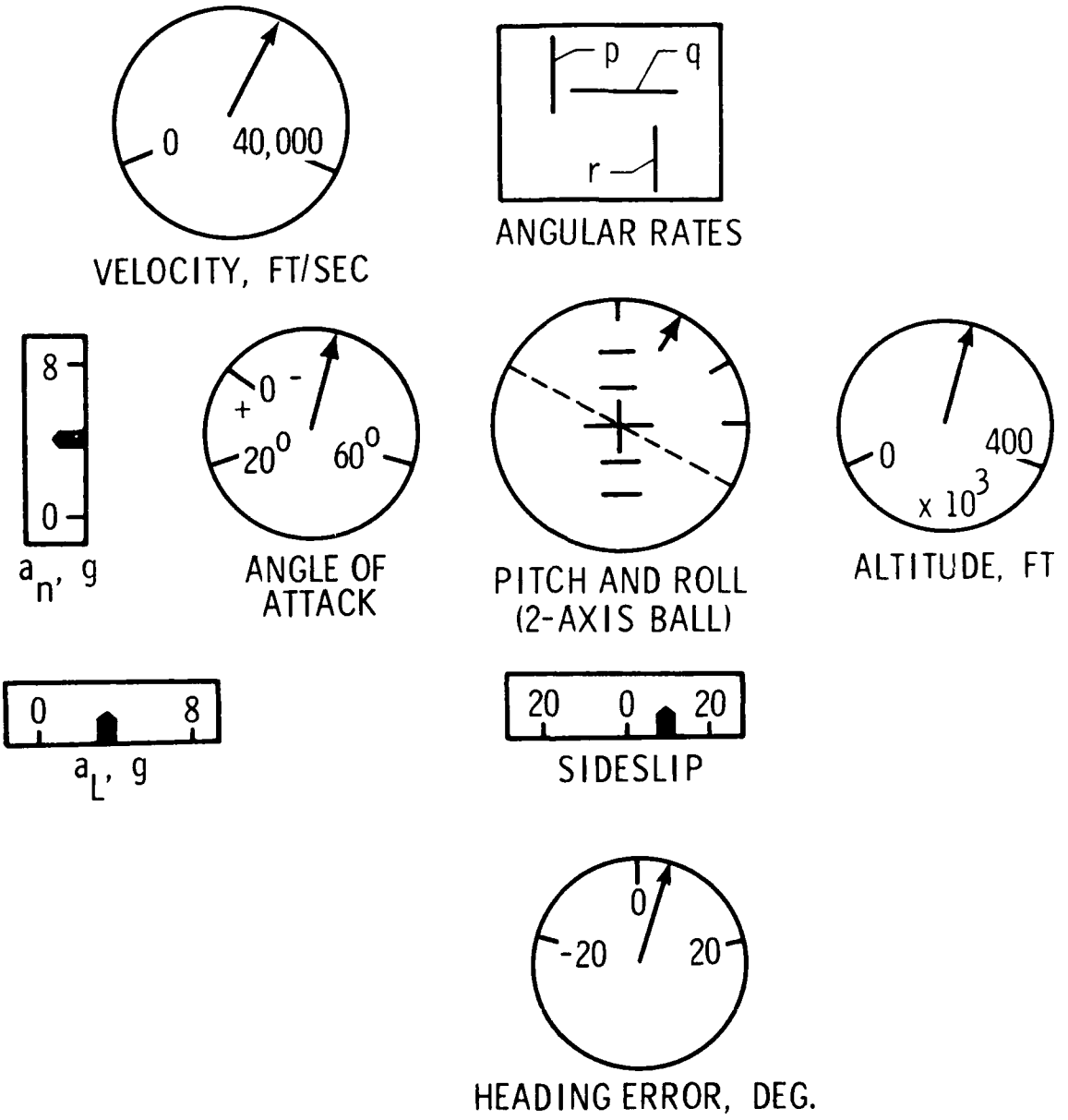

NASA

Figure 13.- Pilot instrument panel.

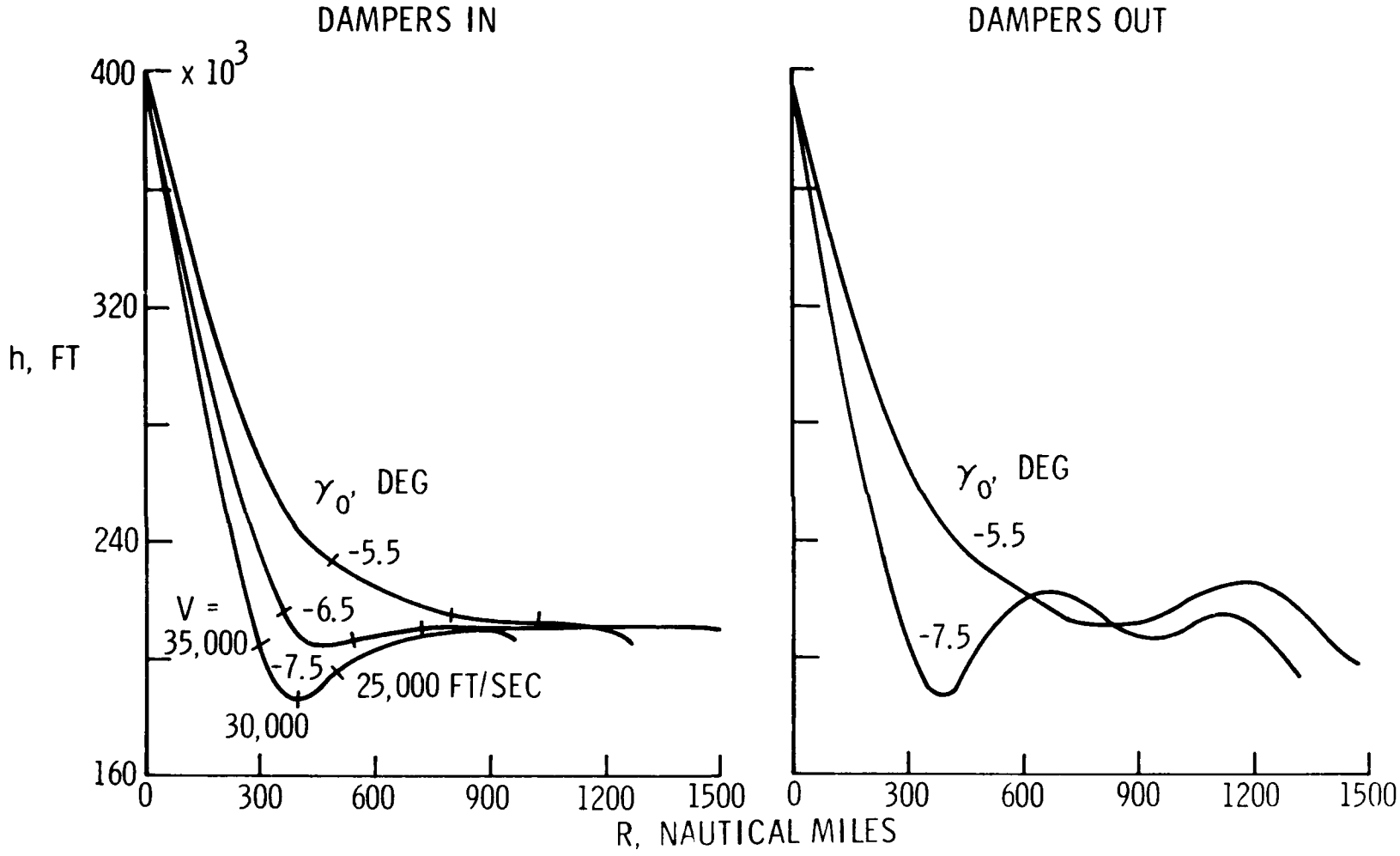

NASA

Figure 14.- Piloted pull-up maneuver with damper effects. $(L/D)_{max} = 0.5$.

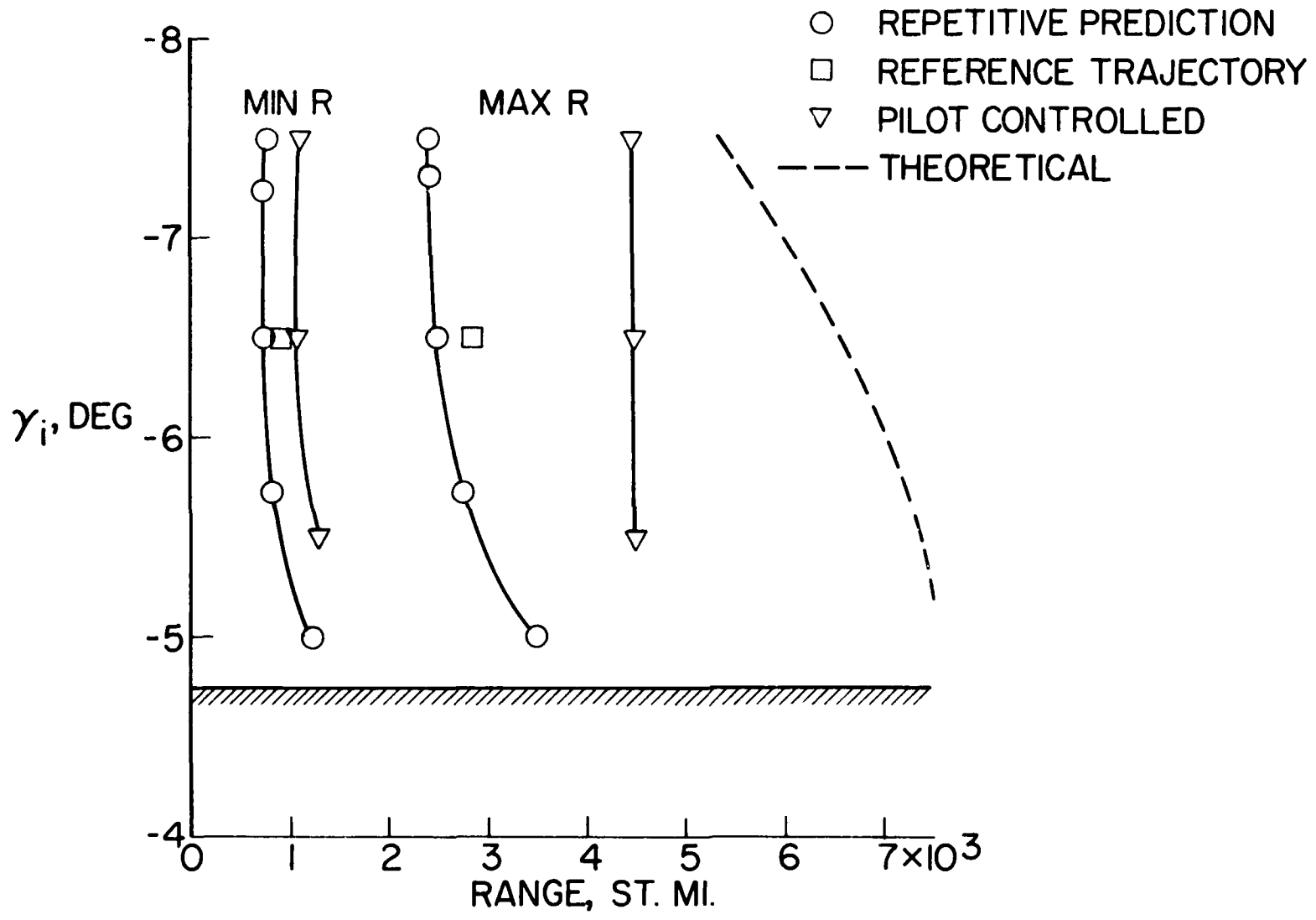

NASA

Figure 15.- Comparison of longitudinal range capability for several guidance systems. $(L/D)_{max} = 0.5$.